Phototroph-heterotroph interactions during growth and long-term starvation across *Prochlorococcus* and *Alteromonas* diversity

Osnat Weissberg*, Dikla Aharonovich* and Daniel Sher

Department of Marine Biology, Leon H. Charney School of Marine Sciences, University of Haifa, Israel

* Dikla Aharonovich and Osnat Weissberg contributed equally to this study

Correspondence: dsher@univ.haifa.ac.il

Running title: *Prochlorococcus-Alteromonas* interactions across diversity

Abstract

Interactions among microorganisms are ubiquitous, yet to what extent strain-level diversity affects interactions is unclear. Phototroph-heterotroph interactions in marine environments have been studied intensively, due to their potential impact on ocean ecosystems and biogeochemistry. Here, we characterize the interactions between five strains each of two globally abundant marine bacteria, *Prochlorococcus* (a phototroph) and *Alteromonas* (a heterotroph), from the first encounter between individual strains and over more than a year of subsequent co-culturing. *Prochlorococcus-Alteromonas* interactions affected primarily the dynamics of culture decline, which we interpret as representing cell mortality and lysis. The shape of the decline curve and the carrying capacity of the co-cultures were determined by the phototroph and not the heterotroph strains involved. Comparing various models of culture mortality suggests that death rate increases over time in mono-cultures but decreases in co-cultures, with cells potentially becoming more resistant to stress. During 435 days of co-culture, mutations accumulated in one *Prochlorococcus* strain (MIT9313) in genes involved in nitrogen metabolism and the stringent response, indicating that these processes occur during long-term nitrogen starvation. Our results suggest potential mechanisms involved in long-term starvation survival in co-culture, and highlight the information-rich growth and death curves as a useful readout of the interaction phenotype.

Keywords: Microbial interactions, growth curves, machine learning, mortality, co-culture

Introduction

Interactions among microorganisms occur in every known ecosystem. Positive (synergistic) interactions allow organisms to exchange resources, potentially increasing biodiversity, whereas negative interactions such as competition, allelopathy and predation may lead to organisms displacing one another (recently reviewed by (Fritts et al., 2021; Gralka et al., 2020)). Detailed studies of the interactions between selected model organisms (often in laboratory co-cultures) have begun to reveal the diversity of molecular mechanisms whereby organisms interact with each other (Fritts et al., 2021; Harrington et al., 2021; Weisskopf et al., 2021). However, it is currently unknown to what extent the studied interactions are conserved across organisms, growth stages or environmental conditions. For example, while broad-scale phylogenetic patterns are often observed in microbial interactions, closely related bacteria may differ in the way they interact with other organisms, likely as a result of the significant genetic diversity observed in many microbial clades (e.g. (Cordero et al., 2012; Long & Azam, 2001)). Additionally, the same pair of interacting organisms can synergize or compete depending on the composition of the culture media and the growth stage of (co)-culture (e.g. (Grossart & Simon, 2007; Segev et al., 2016; Seyedsayamdost et al., 2011). Finally, both the coarse-grained ecological classification of microbial interactions (e.g. positive/negative) and the high-resolution mechanistic view obtained using advanced physiology and omics approaches are difficult to translate into quantitative, predictive models of organismal growth and decline (Antoniewicz, 2020; Gralka et al., 2020; Zoccarato et al., 2020) . Therefore, we still face fundamental challenges in interpreting and understanding the increasingly diverse and mechanistic view of microbial interactions and translating these insights into conceptual and mathematical models of cell growth and death.

Growth curves from batch (co)-cultures are information-rich views of microbial growth and mortality, which can provide an important link between the phenotypic outcome of microbial interactions and the underlying mechanism. Growth curves can be divided into discrete phases (lag, exponential, stationary, decline and long-term stationary phases), and can be used to extract quantitative parameters such as growth rates, lag times, etc. (Sher et al., 2011; Warringer et al., 2008). An extra layer of more subtle information may exist in the shapes of the growth curves, providing hints of important shifts in the physiology of the growing organisms, as classically demonstrated for diauxic growth in *E. coli* (Monod, 1949). Notably, while many studies of bacterial interactions focus on the exponential growth stage or on culture yield at a specific time-point (e.g. (Foster & Bell, 2012; Pacheco et al., 2021; Vetsigian et al., 2011)), fewer studies look at the shape and dynamics of the decline phases, which can provide important hints regarding the effect of interactions on the process of microbial mortality (e.g. (Christie-Oleza et al., 2017; Grossart, 1999; Ratzke & Gore, 2017)).

Here, we explore to what extent intra-clade diversity affects the outcome of microbial interactions, using growth curves as the major phenotypic "readout". Our model organisms are two globally abundant clades of marine bacteria: a cyanobacterial primary producer (*Prochlorococcus*) and a heterotrophic γ-proteobacterium (*Alteromonas*). Interactions between marine phototrophs (phytoplankton, including cyanobacteria) and heterotrophic bacteria have been studied intensively, as phytoplankton are responsible for about one-half of the photosynthesis on Earth (e.g. (Cirri & Pohnert, 2019; Cole, 1982; Field et al., 1998; Ramanan et

al., 2016; Seymour et al., 2017)). Thus, phytoplankton-bacteria interactions may strongly affect community structure and function on scales from microns to thousands of kilometers (Hennon et al., 2018; J. Jeffrey Morris et al., 2012). Our model primary producer, *Prochlorococcus*, is found throughout the euphotic zone, the sunlit upper portion of the ocean. There are multiple *Prochlorococcus* clades, broadly partitioned into high-light (HL) and low light (LL) adapted ecotypes, which differ in their photosynthetic parameters and occupy different niches in the ocean (surface vs deep water, reviewed by (Biller et al., 2015)). Strains differ also in traits such as the capacity to utilize different forms of inorganic nutrients and organic matter, as well as in their interactions with heterotrophic bacteria and phage. *Alteromonas* is a clade of free-living marine bacteria, which are also partitioned into surface and deep groups (*A. macleodii* and *A. mediterranea*, respectively) (López-Pérez & Rodriguez-Valera, 2016). *Alteromonas* strains also exhibit diverse capabilities to utilize carbohydrates, acquire iron and in motility (Koch et al., 2020). Interactions between individual strains of *Prochlorococcus* and *Alteromonas* have been characterized in some detail (Aharonovich & Sher, 2016; Diner et al., 2016; Hennon et al., 2018; Hou et al., 2018; J. J. Morris et al., 2011; Roth-Rosenberg et al., 2020; Sher et al., 2011). While the phenotype and gene expression patterns during interactions vary between strains, this variability has not been explored systematically (Aharonovich & Sher, 2016; Biller et al., 2016; Sher et al., 2011). Notably, strain- and condition-dependent phytoplankton-heterotroph interactions are observed also in other systems, including *Synechococcus*, a close relative of *Prochlorococcus* (Christie-Oleza et al., 2017; Zheng et al., 2020), as well as eukaryotic microalgae (e.g. coccolithophores and diatoms, (Amin et al., 2015; Grossart & Simon, 2007; Segev et al., 2016; Seyedsayamdost et al., 2011)).

We characterized the interactions between five strains each of *Prochlorococcus* and *Alteromonas*, from the first encounter between previously-axenic strains (i.e., grown in mono-culture) and over up to 435 days of co-culture (25 phototroph-heterotroph combinations across ~1.2 years, Fig 1a, Fig S1). The culturing period spanned multiple cycles of exponential growth, culture decline and long-term nitrogen starvation (Roth-Rosenberg et al., 2020). Nitrogen stress or starvation occurs across wide swaths of the global ocean, and affects a significant fraction of the *Prochlorococcus* diversity (Saito et al., 2014; Ustick et al., 2021). We focused our analysis on *Prochlorococcus* growth and decline, which is easily measured using bulk culture fluorescence in a non-invasive manner (e.g. (Coe et al., 2016; Sher et al., 2011). Using this dataset of 429 growth curves, as well as associated cell number measurements and genome resequencing, we ask: i) How do the interactions between *Prochlorococcus* and *Alteromonas* vary across the diversity of each organisms? ii) Do the interactions change over time (i.e. do the organisms adapt to "living together")? iii) When, during the life-cycle of a *Prochlorococcus* batch culture, do microbial interactions have the largest impact on growth and death, and can this impact be quantified? iv) Can the combination of growth curves, cell counts and genomic data provide hints as to which potential metabolic pathways are affected by the long-term interactions?

118 ## Results and Discussion

119 ### Differences in co-culture phenotype are related to *Prochlorococcus* but not
120 ***Alteromonas* strains**

121 The axenic cultures and the co-cultures differed primarily in their decline stage, and this was
122 observed already from the first encounter between previously-axenic *Prochlorococcus* and
123 *Alteromonas* (Experiment 1). In experiment 1, all co-cultures and axenic controls grew
124 exponentially (Fig 1a, b). However, all axenic cultures showed a rapid and mostly monotonic
125 decrease in fluorescence starting shortly after the cultures stopped growing, reaching levels
126 below the limit of detection after ~20-30 days. In contrast, the decline of co-cultures rapidly
127 slowed, and in some cases was interrupted by an extended "plateau" or second growth stage (Fig
128 1b). Across multiple experiments, 92% of the co-cultures contained living cells for at least 140
129 days, meaning that they could be revived by transfer into fresh media. In contrast, none of the
130 axenic cultures were able to re-grow when transferred into fresh media after 60 days (Fig 1a, Fig
131 S1). These results are consistent with previous studies of *Prochlorococcus* (Roth-Rosenberg et al.,
132 2020) and *Synechococcus* (Christie-Oleza et al., 2017). Similarly, it has previously been shown that
133 *Prochlorococcus* MIT9313 is initially inhibited by co-culture with *Alteromonas* HOT1A3, while
134 MED4 is not (Aharonovich & Sher, 2016; Sher et al., 2011). This "delayed growth" phenotype was
135 observed here too, was specific to MIT9313 (not observed in other *Prochlorococcus* strains) and
136 occurred with all *Alteromonas* strains tested (Fig 1b).

137

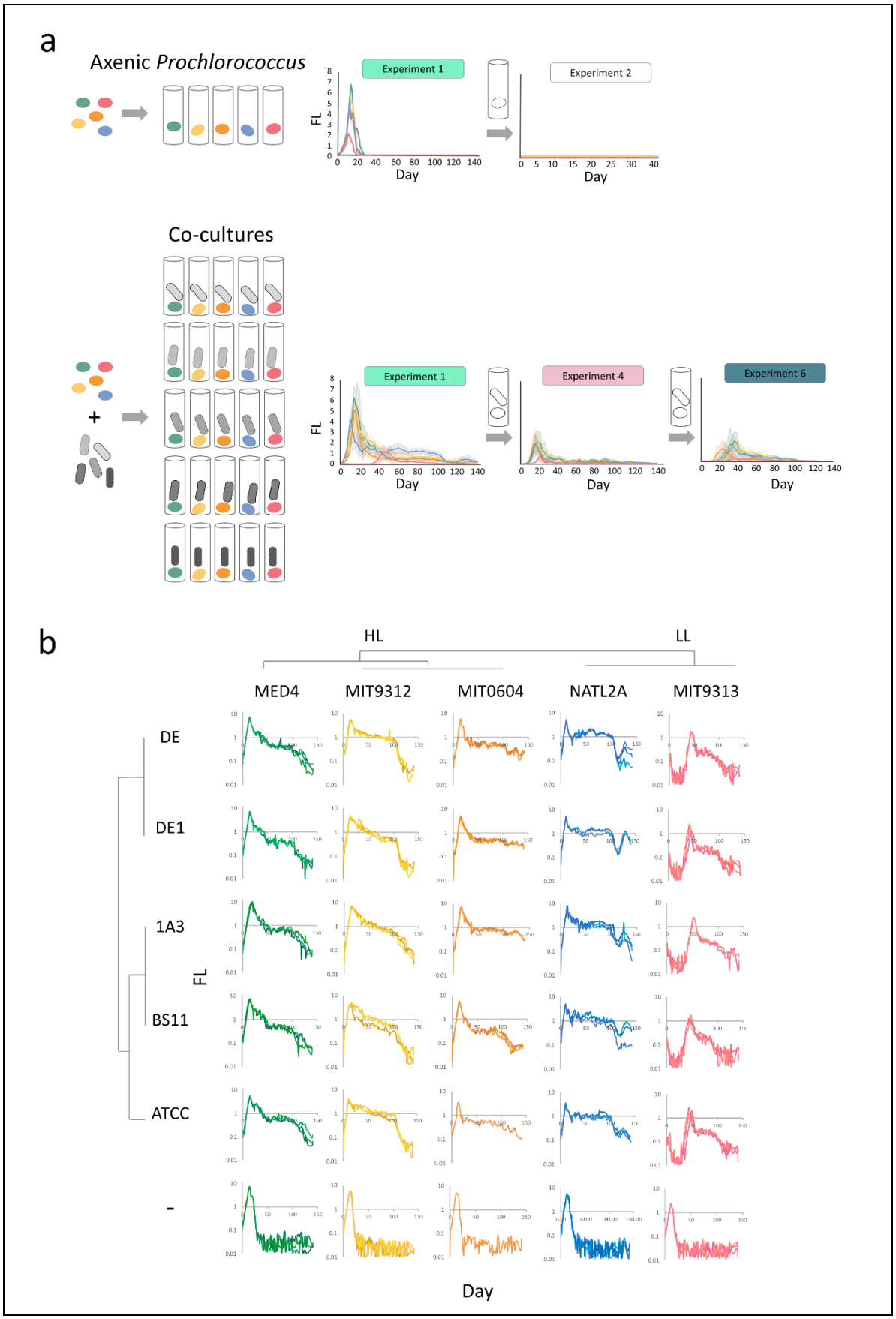
a
Axenic Prochlorococcus
Experiment 1
Experiment 2
FL
Day
Co-cultures
Experiment 1
Experiment 4
Experiment 6
FL
Day
b
HL
LL
MED4
MIT9312
MIT0604
NATL2A
MIT9313
DE
DE1
1A3
BS11
ATCC
-
FL
Day

Fig 1: Overview of the dynamics of *Prochlorococcus-Alteromonas* co-cultures from first encounter and over multiple transfers. a. Mean growth curves of the five *Prochlorococcus* strains over multiple cycles of exponential growth, culture decline and long-term starvation. The top row shows the transfer of axenic strains from experiment 1 after 60 days, with no subsequent growth observed. The bottom row shows the transfer of co-cultures from experiment 1 after 100 days (experiment 4) and additional transfer after 140 days (experiment 6), with subsequent growth. Shaded areas indicate standard error. b. High reproducibility and strain-specific dynamics of the initial contact between *Prochlorococcus* and *Alteromonas* strains (experiment 1). Three biological replicates for each mono-culture and co-culture are shown.

138

139 A visual inspection of the growth curves in Fig 1b suggested subtle yet consistent differences in
140 the shape of the growth curve, and especially the decline phase, between different
141 *Prochlorococcus* strains. To test this, we used the growth curves as input for a Principal
142 Component Analysis (PCA), revealing that the growth curves from each *Prochlorococcus* strain
143 clustered together, regardless of which *Alteromonas* strain they were co-cultured with (Fig 2). The
144 growth curves of all high-light adapted strains (MED4, MIT9312 and MIT0604) were relatively
145 similar, the low-light I strain NATL2A was somewhat distinct, and the low-light IV strain MIT9313
146 was a clear outlier, consistent with this strain being the only one initially inhibited in all co-
147 cultures. This strain (MIT9313) stands out even when the impact of growth timing and magnitude
148 was removed by performing the ordination after scaling and aligning the growth times. The
149 survival of *Prochlorococcus* after extended nitrogen starvation and the clustering of the growth
150 curves by *Prochlorococcus* but not *Alteromonas* strains were observed also in multiple subsequent
151 transfers into fresh media, and are thus robust to the time in co-culture and the initial cell
152 densities (Supplementary text S1).

153 MIT9313 belongs to the low-light adapted clade IV (LLIV), which are relatively distant from other
154 *Prochlorococcus* strains and differ from them in multiple physiological aspects including the
155 structure of their cell wall (Ting et al., 2007), the use of different (and nitrogen-containing)
156 compatible solutes (Klähn et al., 2010) and the production of multiple peptide secondary
157 metabolites (lanthipeptides,(Cubillos-Ruiz et al., 2017; Li et al., 2010)). LLIV cells also have larger
158 genomes, and are predicted to take up a higher diversity of organic compounds such as sugars
159 and amino acids (Yelton et al., 2016). It is intriguing that this strain, which has higher predicted
160 metabolic and regulatory flexibilities (Kettler et al., 2007), differs from all other *Prochlorococcus*
161 strains in the phenotype of co-culture and is the only one initially inhibited in co-culture with
162 *Alteromonas*.

163

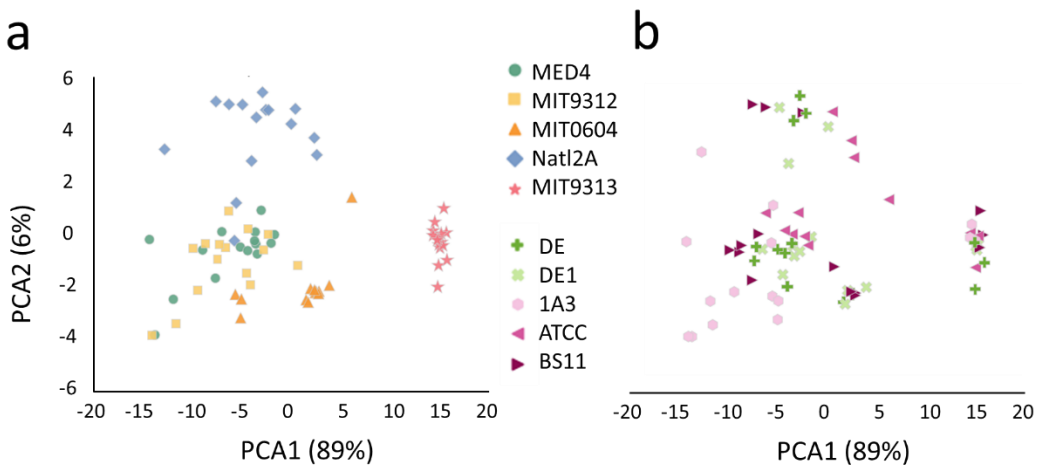

Fig 2: Principal component analysis (PCA) of the growth curves from all co-cultures during 140 days of experiment 1. The ordination is colored by *Prochlorococcus* (a) and by *Alteromonas* (b) strains. The growth curves cluster by *Prochlorococcus* strain (Adonis test, F(4,68) = 80.425, p = 0.001) and not by *Alteromonas* strain (Adonis test, F(4,68) = 1.69, p = 0.17)

The differences between *Prochlorococcus* strains are most evident in the decline and long-term starvation stages

We next used Random Forest Classification to quantitatively determine which stages of the co-culture were most different between the *Prochlorococcus-Alteromonas* pairs. The algorithm accurately predicted, from the growth curves, the *Prochlorococcus* strain (10x cross validation accuracy 0.92±0.17). However, it performed much more poorly when trying to predict the *Alteromonas* strain (accuracy 0.62 ± 0.58) (Fig S4a), providing further support to the observation from the PCA in Fig 2 that the shape of the growth and decline curves was driven by the specific *Prochlorococcus* strain and not by the *Alteromonas*. The classification of the *Prochlorococcus* strains relied heavily on days during the decline phase, as these times had the highest Random Forest feature importance, in agreement with the visual inspection of the growth curves (Fig S4b). Similar results were obtained in all subsequent transfers (Supplementary text S1, Fig S4a).

Focusing on the decline stage, we asked whether the differences in growth curves during long-term co-culture represent differences in the number of cells. This is because physiological differences such as in the amount of chlorophyll per cell, or the fraction of chlorotic *Prochlorococcus* cells, could also affect the growth curves (Coe et al., 2016; Roth-Rosenberg et al., 2020). Flow cytometry counts during the decline stage (after 60, 100 and 140 days) revealed a decrease in the number of *Prochlorococcus* cells over time (Fig 3a), yet the number of cells in the co-cultures was still 3-4 orders of magnitude higher than in the axenic cultures (Fig S5). This is consistent with the growth curves (Fig 1). The number of *Alteromonas* cells also declined with time in the co-cultures (Fig 3a), but the difference between the axenic cultures and the co-cultures was much less pronounced than in *Prochlorococcus* (up to ~4-5-fold after 100 days, Fig S5c). This may be due to the ability of *Alteromonas* to utilize the organic carbon from the natural-seawater-

189 based media, in addition to the dissolved organic matter (DOM) produced by *Prochlorococcus*
190 (Pedler et al., 2014).

191 We next asked whether the carrying capacity of the long-term co-cultures, defined as the sum of
192 the concentrations of *Prochlorococcus* and *Alteromonas* cells, depends on the *Prochlorococcus* or
193 the *Alteromonas* strain. Put differently, one could hypothesize that the total number of cells (and
194 hence the carrying capacity) of the co-culture could depend on the photosynthetically-fixed C
195 provided by *Prochlorococcus*, or alternatively on the recycling capacity of the different
196 *Alteromonas* strains. As shown in Fig 3b and 3c, on days 60 and 100, the number of both
197 *Prochlorococcus* and *Alteromonas* cells clustered depending on the *Prochlorococcus* strain
198 (Adonis, $p = 0.001$), but not on the *Alteromonas* strain (Adonis, $p>0.05$). In terms of carrying
199 capacity, there are clear differences between *Prochlorococcus* strains (Fig S6a), but not
200 *Alteromonas* strains (Fig S6b). Interestingly, two of the *Prochlorococcus* strains, MIT9312 and
201 MIT9313 have similar (and lower) carrying capacity. These two strains belong to different
202 ecotypes but were isolated from the same drop of water. Taken together, these results suggest
203 that it is the dynamics of the *Prochlorococcus* strains, including potentially the amount or
204 composition of fixed and released organic C, which determine the total community carrying
205 capacity.

206 By day 140, the cell numbers had declined significantly, and there was no longer a correlation
207 between the number of *Prochlorococcus* and *Alteromonas* cells (Fig 3). This suggests that the
208 system is not in steady state, with a slow yet constant reduction in carrying capacity evident by
209 the decrease in cell numbers. Indeed, the co-cultures did not survive indefinitely - in a subsequent
210 experiment, only 16/30 cultures could be transferred after 195 days (Fig S7a, b), and only 3/75
211 cultures could be transferred after 250 days (Fig S7c). Notably, MIT0604 was the strain most likely
212 to survive transfer after these extended periods, and was also the most abundant strain after 140
213 days (Fig 3b). While we do not currently have an explanation for the higher survival of this strain,
214 it is noteworthy that it is the only strain to utilize nitrate (Hackl et al., 2021).

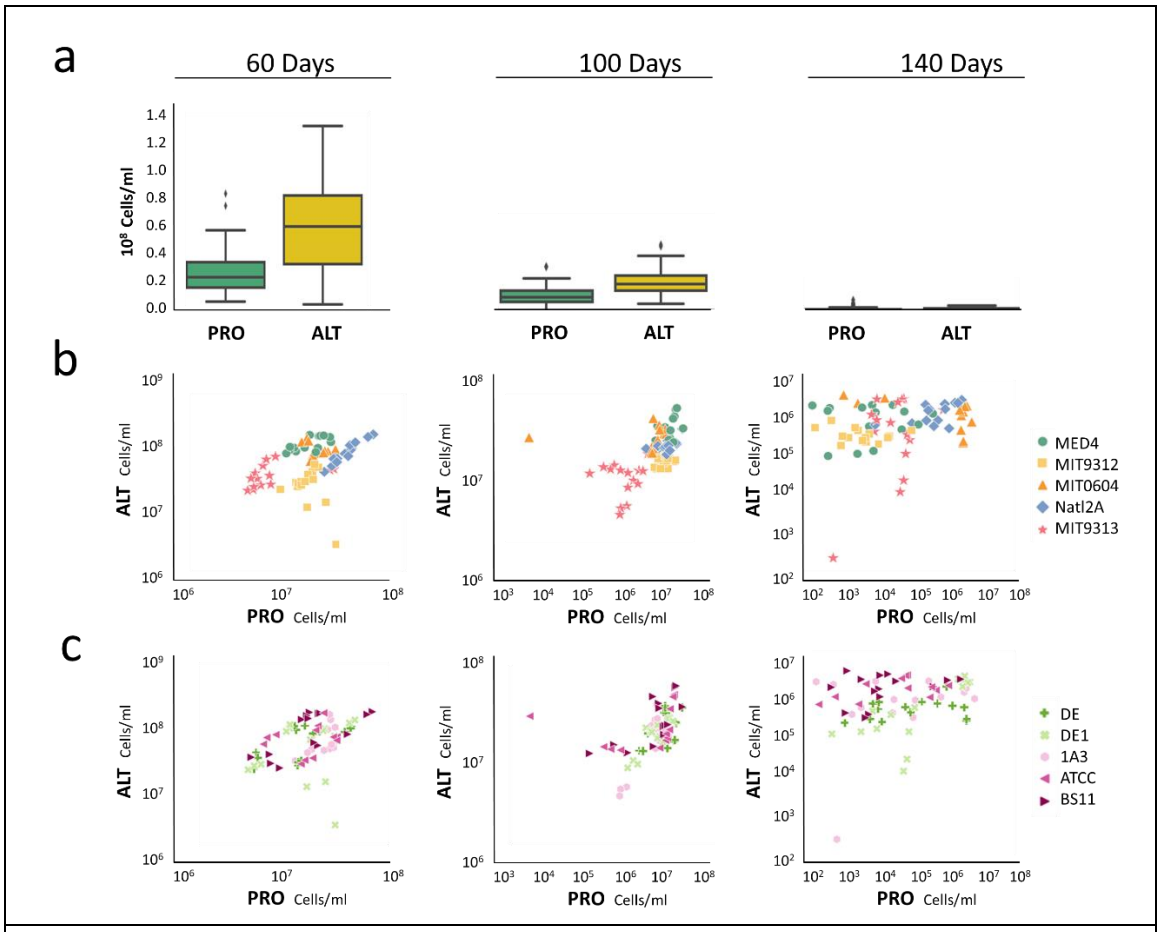

Fig 3: *Prochlorococcus* strain determines the cell numbers of the co-cultures at long term starvation. a. Total co-cultures cell numbers at three different time points, showing a gradual decline. b. *Prochlorococcus* and *Alteromonas* cell numbers, colored by *Prochlorococcus* strain and by *Alteromonas* strain (c) at each time point. Note the clustering of samples based on *Prochlorococcus* but not *Alteromonas* after 60 and 100 days, but not after 140 days.
Results of Adonis test for *Prochlorococcus*:
day 60: $F(4,68) = 32.99$, $p = 0.001$
day 100: $F(4,68) = 28.73$, $p = 0.001$
day 140: $F(4,68) = 16.69$, $p = 0.001$
Results of Adonis test for *Alteromonas*:
day 60: $F(4,68) = 1.599$, $p = 0.149$
day 100: $F(4,68) = 1.998$, $p = 0.074$
day 140: $F(4,68) = 2.212$, $p = 0.043$

Modeling the effect of co-culture on *Prochlorococcus* mortality

Given that the most striking effect of co-culture was on the decline phase of the co-cultures, we asked whether we could quantify this effect, and whether we could identify an appropriate model for mathematically describing culture decline. Importantly, while the growth of bacteria has been extensively studied and modelled, the decline of bacterial cultures, representing bacterial

222 mortality, is much less studied, and mortality is rarely represented in ecological or biogeochemical
223 models of microbial dynamics (Shoemaker et al., 2021). Bacterial mortality has, however, often
224 been modelled in the context of food safety and genome evolution, using either mechanistic or
225 descriptive approaches (Brouwer et al., 2017; Crane & Moore, 1986; Finkel & Kolter, 1999; Patra
226 & Klumpp, 2013; Shoemaker et al., 2021) We chose to focus on four previously-described models
227 which are relatively simple and have a clear biological interpretation (Fig 4a, Table 1). The
228 Exponential model is the simplest and most commonly used one (Pruitt & Kamau, 1993). The Bi-
229 exponential model is slightly more complex, representing two separate subpopulations in the
230 community, each with its own death rate (Crane & Moore, 1986). Weibull model is a probabilistic
231 model, modeling heterogeneous population with a diverse stress tolerance (Shoemaker et al.,
232 2021; Van Boekel, 2002) and finally the Harmonic model employs a quadratic rate of decline which
233 is often associated with predator-prey interaction or encounter rate (Pruitt & Kamau, 1993).
234 When fitting each of these models to the decline phase of the growth curves, the Weibull model
235 stands out as it has a low error for both axenic and co-cultures (Table 1, Fig 4b). Based on this
236 model, and assuming that culture fluorescence is related to the number of non-lysed cells in the
237 media, axenic *Prochlorococcus* cells die more than ten-fold faster than cells in co-culture (2-
238 decimal reduction time, td_2, is 12.58 ± 3.85 days for axenic cultures and 316 ± 337 days for co-
239 cultures).

240

241

242 **Table 1: Mathematical description and biological interpretation of four models used to describe**
243 **bacterial mortality**

Mathematical model	**Derivative**	**# Params**[1]	**Physiological Interpretation**	**Axenic RMSE** [2] **(n=13)**	**Co-culture RMSE (n=343)**	**Reference**
Exponential $X = X_0\, e^{-a\,t}$	$\frac{dX}{dt} = -aX$	1	Constant ratio of the population dies in each time point	0.26 ± 0.11	0.29 ± 0.21	(Pruitt & Kamau, 1993)
Bi-Exponential $X = X_0(f\, e^{-a_1\,t} + (1-f)\, e^{-a_2\,t})$	$\frac{dX}{dt} = -f a_1 X_1 - (1-f)\, a_2 X_2$	3	Two subpopulations with different persistence under stress and death rates	0.26 ± 0.11	0.16 ± 0.12	(Crane & Moore, 1986)
Harmonic $X = X_0\, \frac{1}{1+a\,t}$	$\frac{dX}{dt} = -a\, X^2$	1	Quadratic mortality rate – dependence on cell-cell encounters	0.50 ± 0.19	0.19 ± 0.13	(Pruitt & Kamau, 1993)
Weibull $X = X_0\, e^{-\frac{t^n}{a}}$	$\frac{dX}{dt} = -c\, t^{n-1} X$ *	2	Probabilistic model with a heterogeneous distribution of stress tolerance	0.14 ± 0.08	0.18 ± 0.11	(Van Boekel, 2002)

[1] # Params – number of free parameters

[2] RMSE - Root Mean Square Error

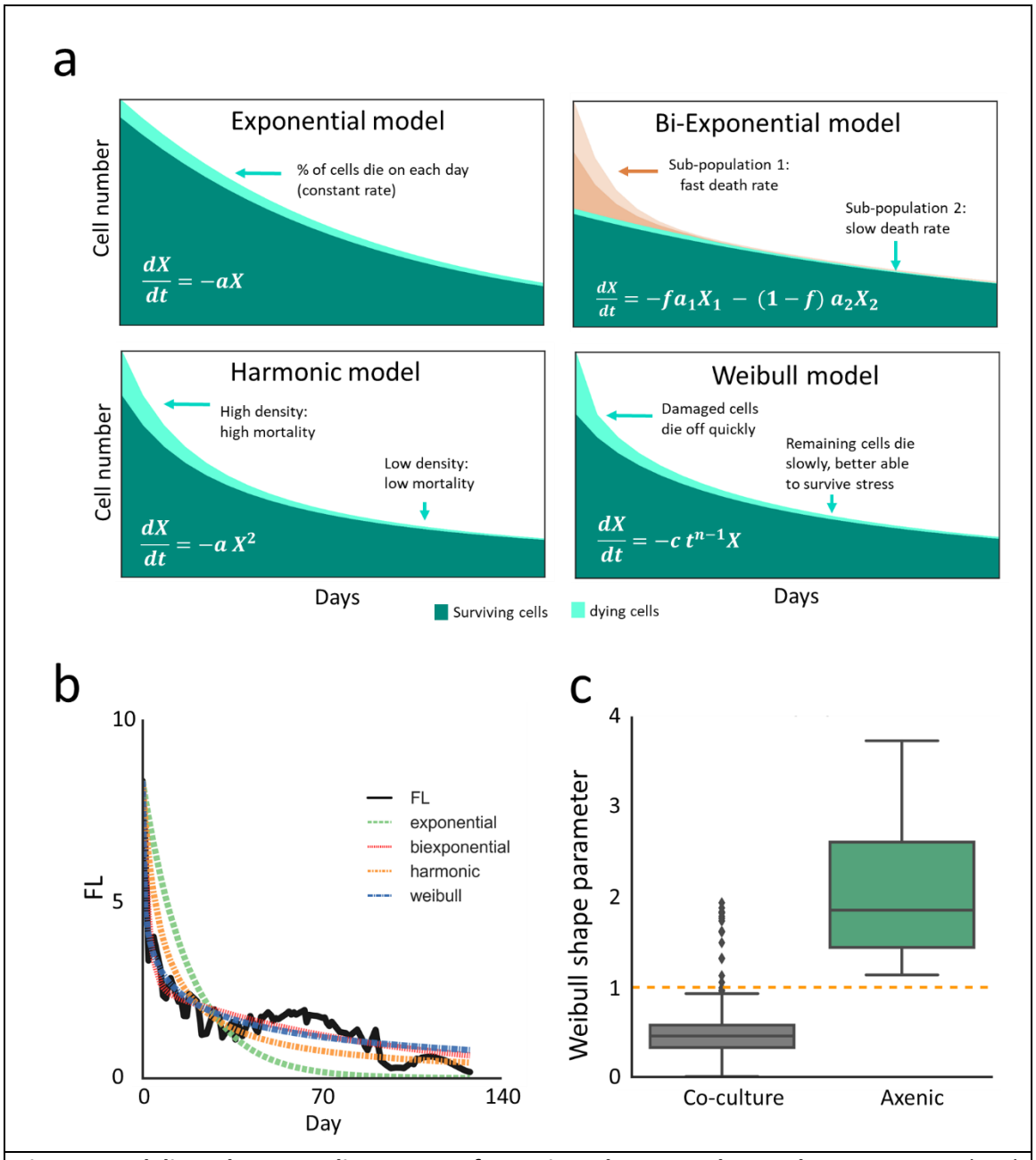

Fig 4: Modeling the mortality stage of axenic cultures and co-cultures. a. Graphical representation of four decline models. The lighter blue or peach colors represent the dying fraction of the population at each time-point. b. Comparison of the four decline models with co-culture of *Prochlorococcus* NATL2A with *Alteromonas* HOT1A3. While the Weibull model provides the best fit (see Table 1), none of the decline models fully describes the complexities of culture decline. c. Weibull Shape parameter (n) in co-cultures vs axenic cultures (student t-test, $p < 0.001$). In all axenic samples $n>1$, and hence the decline rate increases over time. In most co-cultures $n<1$, suggesting that, as the culture declines, the remaining cells are better adapted to stress and thus their death rate decreases.

244

In the Weibull model, the 'shape parameter' (n) represents the change over time in the susceptibility of the bacterial community to stress. A shape parameter above one represents an increasing probability that cells will die as time increases (e.g. due to the accumulation of damage), whereas a shape parameter below one suggests that, over time, the cells become more resistant to damage. Axenic cultures have high shape value of 2.1 ± 0.9, suggesting an accumulation of cell damage leading to increasing death rate, whereas that of co-cultures is 0.5 ± 0.3 (student t-test, $p < 0.001$) (Fig 4c). This suggests that, in contrast to mono-cultures, in each cycle of co-culture the *Prochlorococcus* cells are acclimating over time to the nutrient stress conditions.

While the Weibull model is useful in quantifying mortality rates and raising the hypothesis that *Prochlorococcus* cells are acclimating to starvation over time, none of the tested models was able to fully capture the intricate dynamics of culture decline (Fig 4b). In most co-cultures involving *Prochlorococcus* strains NATL2A, MED4 and MIT0604, culture decline was not monotonic, and was interrupted by a second growth phase about 40-50 days after the cultures started declining. We propose that this "second breath" represents either a consistent shift in the physiology of one of the interacting partners (e.g. by activating pathways for the salvage of previously-exuded DOM) or a change in the availability of labile DOM, e.g. following a period of mortality and lysis of *Prochlorococcus* and/or *Alteromonas*. Because the second growth phase was mostly absent in MIT9312 and MIT9313, we speculate that this phenomenon, too, is driven primarily by the specific strain of *Prochlorococcus* cells in co-culture. Notably, the Weibull model, while best representing the experimental results, is less appropriate for ecological/biogeochemical models, because the time from peak is an inherent part of the differential equation. In such cases, the harmonic model formulation may be more appropriate, as it represents mortality of co-cultures better than exponential decline with the same number of parameters, and quadratic expressions for mortality are already used in such models (Dutkiewicz et al., 2001; S. K. Moore et al., 2006; Murray A.G. and Parslow J.S., 1999).

Accumulated mutations in *Prochlorococcus* suggest a role for nitrogen use and the stringent response

During the experiments described above, we co-cultured strains of *Prochlorococcus*, which had each been previously maintained in axenic mono-cultures for hundreds or thousands of generations. We also exposed these parental strains, which are routinely maintained under conditions of exponential growth, to repeated cycles of growth, mortality and long-term survival under N starvation. To identify whether these shifts in life-style could result in genetic changes in the co-cultured populations, we re-sequenced the genomes of duplicate cultures of *Prochlorococcus* MIT9313 co-cultured with *Alteromonas* HOT1A3 after a total of 435 days in co-culture (including 3 cycles of growth, mortality and survival, Fig 5a, Fig S1). We also re-sequenced the parental strain used in these experiments, which itself had been maintained as an axenic culture for ~16 years since originally being sequenced (Rocap et al., 2003). Since the read coverage for *Alteromonas* was low, we focus here on *Prochlorococcus*.

285 Over the course of 435 days in co-culture (~220 generations), the two replicate MIT9313 co-
286 cultures accumulated 32 and 39 observed mutations in protein-coding genes, compared to 57
287 mutations accumulated in the parental strain over ~16 years of growth at similar maximum
288 population sizes (~2,900 generations, 15-20ml cultures, Fig 5, Fig S8 and File S1). This suggests
289 that, during the repeated cycles of growth, decline and starvation, the mutation rate of MIT9313
290 in co-culture increased roughly 7-9-fold compared to the parental axenic strain growing primarily
291 exponentially (Supplementary text S2). Strikingly, many of the mutations were observed to occur
292 in genes involved in nitrogen utilization and stress responses. Three genes involved in nitrogen
293 metabolism each had two or more mutations associated with them – the nitrite reductase gene
294 nirA and two genes in the operon involved in the production and transport of glycine betaine (Fig
295 5b, c).

296 The parental MIT9313 strain had a frameshift mutation in the N'-terminal reductase domain of
297 nirA, observed in 100% of the sequencing reads, which likely led to a truncated, inactive protein.
298 This frameshift is not found in the evolved strain, after ~220 generations in co-culture. Since nitrite
299 was not added to the (co)-cultures, and the *Alteromonas* genome does not contain the genes for
300 nitrification (the ammonia monoxygenase gene), this raises the question of what are the sources
301 of nitrite that is presumably being utilized by the evolved strain. We provide a speculative answer
302 in Fig 5d. It has previously been shown, in the freshwater cyanobacterium *Phormidium*, that nitrite
303 can be produced by the enzymatic dismutation of hydroxylamine (NH_2OH) in the presence of
304 hydrogen peroxide, H_2O_2 (reaction 3 in Fig 5d, the other product is NH_3 (Bagchi & Kleiner, 1990,
305 1991)). NH_2OH, in turn, can be produced by the peroxidation of glutamine to glutamate (reaction
306 2 in Fig 5d, (Bagchi & Kleiner, 1991)). The H_2O_2 required for these reactions is produced by multiple
307 metabolic reactions in cyanobacteria (Latifi et al., 2009), and it has previously been shown that
308 oxidative stress is enhanced during nitrogen starvation in *Prochlorococcus* (Mcdonagh et al.,
309 2012). Thus, an active nitrite reductase may enable MIT9313 to recycle NH_2OH, produced when
310 the cells are under nitrogen starvation conditions (Fig 5d). Intriguingly, H_2O_2 is also produced
311 during amino acid oxidation, the process in which cells degrade amino acids to obtain N and
312 carbon backbones (e.g. by several types of L-amino acid oxidases, reaction 1 in Fig 5d, (Schriek et
313 al., 2007)). It is currently unclear to what extent these amino acid degradation pathways are
314 present and active in *Prochlorococcus*, as the streamlined genomes of these organisms lack
315 several known enzymes (Gau et al., 2007; Schriek et al., 2007), although we note that a putative
316 L-aspartate oxidase had a non-synonymous mutation in the evolved strains. If, however, nitrogen
317 starvation induces amino acid oxidation and the production of H_2O_2 in *Prochlorococcus*, this would
318 provide a mechanistic explanation for the inability of these organisms to survive long-term N
319 starvation alone (J. Jeffrey Morris et al., 2008, 2012) Further studies are required to test this
320 hypothesis.

321 Three genes in the operon for the production and import of the compatible solute glycine betaine
322 accumulated mutations – the glycine-sarcosine methyltransferase *gsmt*, and two subunits of the
323 glycine-betaine ABC transporter (Fig 5c). None of the mutations occurred in residues known to be
324 important to the activity of these proteins. Under N starvation, it is possibly advantageous for the
325 cells to reduce the production of glycine betaine, which contains N atoms, in favor of other
326 compatible solutes such as sucrose (Klähn et al., 2010). However, during the long experiments
327 described here, it is also likely that the osmotic strength of the growth media increased (due to

328 both cell lysis and the evaporation of water), and this could lead to an increased requirement for
329 glycine betaine (Klähn et al., 2010). Further work is needed in order to differentiate between these
330 two hypotheses. Importantly, glycine betaine provides both carbon (energy) and N to co-occurring
331 bacteria, including SAR11 (Becker et al., 2019). Additional genes involved in N metabolism that
332 accumulated non-synonymous mutations (one for each gene) include enzymes involved in amino
333 acids production or degradation (the L-aspartate oxidase mentioned above, biosynthetic arginine
334 decarboxylase and cysteine synthase) and a putative aminotransferase (Fig 5b, File S1). Genetic
335 changes occurred in additional genes not directly related to nitrogen metabolism, but known to
336 be involved in the nitrogen stress response in cyanobacteria. These include the glycogen synthase
337 gene glgA (Tolonen et al., 2006) as well as genes involved in the synthesis of chlorophyll and other
338 proteins from the photosynthetic apparatus.

339 Finally, the bacterial "alarmone" (p)ppGpp is a master regulator of bacterial stress responses,
340 including the "stringent response" to carbon or amino acid starvation (recently reviewed by
341 (Steinchen & Bange, 2016)). Two mutations were observed in a gene homologous to the relA/spoT
342 bifunctional (p)ppGpp synthase/hydrolase. The product of this gene both activates the stringent
343 response by synthesizing (p)ppGpp from GTP and represses it, by hydrolyzing the alarmone back
344 to GTP (Hogg et al., 2004; Steinchen & Bange, 2016). Both of the mutations were in the hydrolase
345 domain, and one of them (P95T) occurs in a residue which is predicted to take part in Mn
346 coordination in the active site of the enzyme, potentially leading to a hydrolase-incompetent
347 enzyme (Hogg et al., 2004; Steinchen & Bange, 2016). We speculate that this mutant may be
348 deficient in its ability to "turn off" the stringent response, potentially leading to enhanced survival
349 under stress.

350

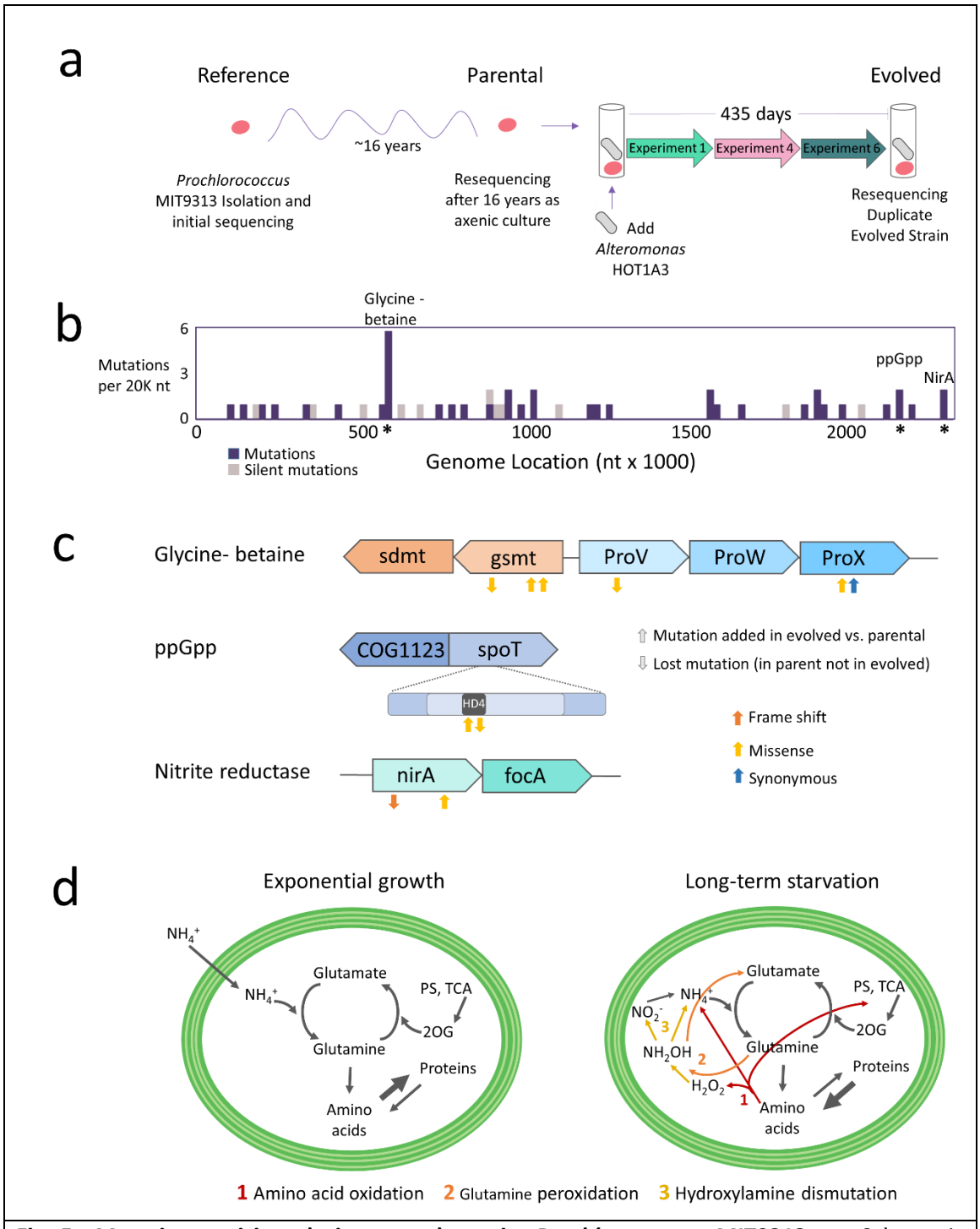

Fig 5: Mutations arising during co-culture in *Prochlorococcus* MIT9313. a. Schematic illustration of resequencing setup. b. Location of accumulated mutations (SNPs or indels) on the MIT9313 genome. Bars represent the number of mutations (changes between the parental and evolved populations) per 20,000 bases in both biological duplicates. Dark purple bars represent non-synonymous mutations; light grey bars represent synonymous mutations. c. Type and location of mutations in genes involved in Glycine-betaine, ppGpp and Nitrite reductase metabolism. The bar below the spoT gene shows the domain structure. d. Schematic diagram of the proposed role of nitrite reductase during long-term starvation in MIT9313. The

suggested pathway leading to the production of nitrite (NO_2^-) through hydroxylamine (NH_2OH) is shown in long term starvation compared to exponential growth. The balanced equations for this pathway are: Reaction 1 - amino acid oxidation by L-amino acid oxidases (e.g. Alanine + H_2O + O_2 -> Pyruvate + NH_4^+ + H_2O_2); Reaction 2 - Peroxidation of glutamine to glutamate ($C_5H_{10}N_2O_3$+H_2O_2->$C_5H_9NO_4$ + NH_2OH); Reaction 3 - Dismutation of hydroxylamine in the presence of H_2O_2 (2NH_2OH + H_2O_2 -> NO_2^- + NH_4^+ + 2H_2O). PS – photosynthesis, TCA - tricarboxylic acid cycle, 2OG - 2-oxoglutarate

Summary and future directions

As our appreciation of the richness and dynamicity of microbial communities increases, so does the understanding that interactions between microorganisms are critical to the structure and function of these communities. Elucidating the roles of microbial interactions requires both well-characterized model organisms and a way to extend the insights from such models across the diversity of organisms and environmental conditions. Our results from the highly-simplified system of multiple *Prochlorococcus* and *Alteromonas* strains provide an important step towards this goal. Using the rich information on interaction phenotypes present in the growth and decline curves, we identify conserved and strain-specific facets of these interactions. Despite the genetic diversity across the *Alteromonas* strains studied, it was the identity of the *Prochlorococcus* strain that determined the interaction phenotype. This manifests in the growth and decline rates, in the shape of the curve (primarily the decline phase), and in the number of cells living in long-term, nitrogen-starved co-culture. Testing multiple mathematical models of culture decline suggests that cells in axenic cultures are accumulating damage and dying more rapidly over time, while cells in co-culture are acclimating, likely changing their physiology and also evolving to better deal with the emergent stress. Comparing the modelled and observed curves allows for the identification of consistent and reproducible shifts in physiology, for example the "second breath" of growth followed by rapid decline in NATL2A co-cultures (Fig 4b), that can then be studied in-depth.

Under our laboratory conditions, it is likely that nitrogen starvation is the main selection force driving the phenotypic outcome of long-term co-cultures, although other stressors such as the increase in osmolarity/salinity or the accumulation of waste products cannot be ruled out. We speculate that the genetic changes observed in the MIT9313 population are primarily indicative of processes occurring in the *Prochlorococcus* cells due to nitrogen starvation and/or osmotic stress, rather than representing a direct response to the interactions with *Alteromonas*. It is possible that a major effect of co-culture with *Alteromonas* is to slow down the deterioration in *Prochlorococcus* homeostasis, providing a "buffer" that enables *Prochlorococcus* to activate its own starvation survival responses, and subsequently to genetically evolve. *Alteromonas* may similarly allow *Prochlorococcus* to adapt to light starvation (Coe et al., 2016), yet the genetic mechanisms underlying this survival remain unclear (Coe et al., 2020). However, the buffering effect of *Alteromonas* cannot be taken for granted, as it also depends on culture conditions, for example CO_2 concentrations (Hennon et al., 2018).

Once mortality has been slowed down enough to allow acclimation and/or adaptation, the differences in the resulting shape of the co-culture curves are likely due to strain-specific

differences in nitrogen metabolism. For example, *Prochlorococcus* MIT9313 produces glycine betaine as a compatible solute (unlike MIT9312 and NATL2A (Klähn et al., 2010)), and it is possible that producing large amounts of this N-containing molecule constrains the metabolic responses of this strain to N starvation differently from other strains, resulting in this strain having a distinct phenotype. The reasons for the differences between the other *Prochlorococcus* strains are less clear, but may be related to differences in the regulatory networks (e.g. those affected by the ppGpp alarmone) or the capacity to utilize organic substances released by *Alteromonas* (Yelton et al., 2016). Some of the mutations were in hypothetical genes and in some cases in multiple hypothetical genes in the same putative operon (e.g. PMT1541 and PMT1542). Future work is needed to determine whether these represent "internal" *Prochlorococcus* processes, or whether they are part of the tools used by *Prochlorococcus* to interact with co-occurring bacteria.

Why is it the identity of the primary producer (*Prochlorococcus*) rather than the heterotrophic "recycler" (*Alteromonas*) that determines the outcome of the co-culture? *A-priori*, it was reasonable to assume that the co-culture phenotype would be affected by the differences between the *Alteromonas* strains in their ability to degrade and utilize polysaccharides and a variety of other organic molecule (Koch et al., 2019, 2020). We speculate that the growth of *Alteromonas* in the co-cultures is fueled primarily by the availability of major biomass components released by *Prochlorococcus* as they die, such as proteins, amino acids and nucleotides. Such common macromolecules do not require highly specialized metabolic processes to degrade and utilize, and hence could be utilized by all of the *Alteromonas* strains. It is possible that the differences between *Alteromonas* strains may manifest when more complex macromolecules are available, e.g. from plant material, or when all of the "easy to digest" (labile) organic matter has been utilized and only complex macromolecules remain (Teeling et al., 2012). These conditions may not have been met in our experiments. Regardless of the underlying mechanism, identifying to what extent the interaction phenotype is dependent on the identity of each of the interacting organisms requires an experimental setup spanning the diversity of both.

Our results identify patterns in the interactions between clades of abundant marine phototrophs and heterotrophs, including consistent shifts in physiology occurring after extended time in co-culture. The mechanistic basis of these shifts in physiology can now be studied in-depth. Given that these shifts occur under conditions where nutrients are scarce and their availability likely depends on recycling between phototrophs and heterotrophs, it is tempting to speculate that such mechanisms may be physiologically relevant in the oligotrophic ocean, much of which is N-stressed (Ustick et al., 2021). Nevertheless, the co-cultures did not reach a steady state, and did not represent a closed system. Thus, processes not represented in these simplified laboratory co-cultures, are necessary to explain the long-term stability over decades of *Prochlorococcus* in the oceans (Malmstrom et al., 2010). Such processes could include multi-organism interactions, as natural communities are much more complex than the laboratory co-cultures, as well as oceanographic processes such as nutrient injection through deep mixing. More generally, cell mortality is intimately linked with the amount and type of recycled organic matter, yet the rate of mortality in natural communities is highly unconstrained (Beckett et al., 2021). Hence, better representation of mortality in mathematical models (e.g. the use of appropriate mortality formulations) is likely important for understanding biogeochemical cycles (Beckett et al., 2021). Finally, this study is a reminder that bacterial growth curves represent an information-rich

429 representation of the life and death of cells, which can be mined to identify potential physiological
430 changes of ecological relevance.

431

432 Materials and Methods

433 Strains and experiment set up

434 Axenic *Prochlorococcus* strains MED4, MIT9312, MIT0604, Natl2A and MIT9313 were maintained
435 in Low N Pro99 media, based on natural sea water, with the addition of 100 µM nitrogen, 50 µM
436 phosphorus and trace metal elements. Under these conditions, *Prochlorococcus* enter stationary
437 stage due to the depletion of NH_4 from the media and nitrogen starvation (Grossowicz et al.,
438 2017). *Alteromonas* strains HOT1A3, Black sea 11, ATCC27126, AltDE1 and AltDE were maintained
439 in ProMM media. both under constant cold while light (27 $\mu Em^{-2} s^{-1}$) at 22ºC in (L. R. Moore et al.,
440 2007; Sher et al., 2011)). Prior to the experiment, the axenicity of the *Prochlorococcus* cultures
441 was tested by inoculating 1 ml culture into 15 ml ProMM (L. R. Moore et al., 2007)). At the start
442 of each co-culture experiment, *Alteromonas* cells from stationary-stage cultures (24-72 hour old)
443 were centrifuged (15 minutes, room temperature, 15,000g), the growth media decanted, and the
444 cells re-suspended in Pro99. The *Prochlorococcus* cultures (growing exponentially) and the re-
445 suspended *Alteromonas* cells were then counted using BD FACSCanto™ II Flow Cytometry
446 Analyzer Systems (BD Biosciences). For each co-culture, $1x10^6$ *Prochlorococcus* cells mixed with
447 $1x10^7$ *Alteromonas* cells. For mono-cultures, $1x10^6$ and $1x10^7$ were added for *Prochlorococcus* and
448 *Alteromonas*, respectively. The experiment was performed using triplicate 20ml cultures in
449 borosilicate test tubes (2.5cm diameter, 15cm length).

450

451 Fluorescence and Flow cytometry

452 Bulk chlorophyll fluorescence (FL) (ex440; em680) was measured almost daily using a
453 Fluorescence Spectrophotometer (Cary Eclipse, Varian). Samples for flow cytometry were taken
454 for cell numbers after 60, 100 and 140 days of experiment 1 (Fig S1). Samples were fixed with
455 glutaraldehyde (0.125% final concentration), incubated in the dark for 10 min and stored in -80
456 °C until analysis. Then, samples were thawed at room temperature and run on a BD FACSCanto™
457 II Flow Cytometry Analyzer Systems (BD Biosciences). To each sample, 2 µm diameter fluorescent
458 beads (Polysciences, Warminster, PA, USA) were added as an internal standard. At first, the
459 natural fluorescence of the cells (chlorophyll pigments) was examined to identify *Prochlorococcus*,
460 identified based on the PerCP-A and FSC-H. Samples were then stained with SYBR Green I
461 (Molecular Probes/ ThermoFisher) to a final concentration according to the manufacturer's
462 instructions and the *Alteromonas* was counted. Data were acquired and processed with FlowJo
463 software. Flow rates were determined several times during each running session, and the average
464 value for a specific run was used for calculating cells per ml.

465

466 PCA ordination

PCA ordination was run on the growth curves. The Cumulative sum of Fluorescence measurements were standardized via standard scalar by subtracting the mean and scaling to unit variance of each feature. Ordination was computed via principal component analysis (PCA). Data preprocessing was done by pandas (0.25.0). Scaling and PCA was done using sklearn (0.21.2).

Growth rate

Growth was computed - by solving the equation:

$$N_t = N_0 \, e^{\mu(t-L)}$$

Where N_t represents the number of cells at time *t*, N_0 is the initial number of cells, μ is the growth rate, and *L* is the growth lag. The LAN transformed equation was used to compute growth rate:

$$\ln(N_t) = \ln(N_0) + \mu(t - L)$$

Linear regression was run on the growth phase, predicting $\ln(N_t)$ based on time *t* with $R^2 > 0.9$. The growth rate μ is the regression coefficient.

Fit to Decline models

The following functions were used to fit against the measured fluorescence:

Exponential: $FL_t = FL_{max} \, e^{-a(t-t_{max})}$

Bi-exponential: $FL_t = FL_{\max}(f \, e^{-a_1(t-t_{max})} + (1-f) \, e^{-a_2 \, (t-t_{max})})$

Harmonic: $FL_t = FL_{\max} \frac{1}{1+a\,t}$

Weibull: $FL_t = FL_{\max} \, e^{-a\,t^n}$

Where FL_t is the Fluorescence measured at time *t*, FL_{max} is the maximum fluorescence measured, t_{max} is the time when the fluorescence was highest, and *a, a1, a2, n, f* are the model parameters estimated by the fitting function.

The decline function was fit against each growth curve via curve_fit() function from scipy package (1.3.0), using the parameters: method='dogbox', loss='soft_l1', f_scale=0.1. Each model was fit using random initial parameter values and the initial values of 0.5 per parameter, and the fit with the lowest RSME selected. Goodness of fit was measures using root mean square error (RMSE).

In the Weibull model the time needed to reduce the population by *d* factors of 10 (t_{d2}) was estimated as in (Van Boekel, 2002), using the formula:

$$t_d = a \, (-ln(10^{-d})^{\frac{1}{n}})$$

495 **Random Forest Classification**

496 Random Forest Classification was run on the growth curves. To detect difference in the curve
497 pattern and not timing specific differences, the curves were aligned such that max growth point
498 are at time zero, and time points from 10 days prior to max growth to 80 days after were selected.
499 Since the specific measurement time points were different in different experiments and samples,
500 rolling average was used to get mean fluorescence per day, and interpolation used to fill in missing
501 measurements. The Fluorescence measurements were standardized via standard scalar by
502 subtracting the mean and scaling to unit variance of each feature. Random Forest model was run
503 in 10x cross validation to classify the curves by *Prochlorococcus* and by *Alteromonas* strains. To
504 find the most significant days in *Prochlorococcus* classification, the model was built 30 times and
505 the mean importance of all features (i.e., measurement days) calculated. Data preprocessing was
506 done by pandas (0.25.0). Scaling and model fitting using sklearn (0.21.2).

507 **Statistics**

508 Statistics were computed using the statsmodels package in python. Multi test correction was done
509 by t_test_pairwise() using Bonferroni correction. Permanova analysis by adonis2 from R vegan
510 package (R 3.61, vegan 2.5-7).

511 **DNA extraction, genome resequencing and SNP analysis**

512 Samples for genomic DNA sequencing was collected from parental strains, before experiment 1
513 and after 435 days from co-cultures (Fig S1, Fig 5a). Samples collected on a 0.22 µm filter (Supor,
514 Pall Corporation), filled with 1 ml of storage buffer (40 mM EDTA, 50 mM Tris pH=8.3, 0.75 M
515 Soucrose) and stored at −80°C. Before extraction samples were thawed on ice and storage buffer
516 removed carefully. DNA extracted using DNeasy PowerWater Kit (Qiagen) according to the kit's
517 protocol. DNA samples (minimum concentration of 1ng/uL) were submitted to the MIT
518 BioMicroCenter in 96 well plate format. Samples were prepared for sequencing using Nextera
519 flex preparation for intact DNA (high throughput) and a size selection of 300-600bp. DNA was
520 sequenced using MiSeq flowcell (v3, 600nt). The samples have been processed using the
521 BMC/BCC 1.7 pipeline updated on 01/11/2019. The NexteraPE adapter and the first 20 bases were
522 trimmed by trimmomatic 0.39-1. And quality checked using fastqc and multiqc. All samples were
523 mapped to the reference genome and variant called using snippy (based on bwa mem mapping,
524 freebayes variant call, snpEff annotation). *Alteromonas* reads were removed from Co-culture
525 samples by first mapping to *Alteromonas* HOT1A3 (NCBI accession: NZ_CP012202.1,
526 NZ_CP012203.1), then running snippy a second time on reads that were not mapped to
527 Alteromonas, mapping against *Prochlorococcus* MIT9313 (NCBI accession: NC_005071.1). The
528 number of reads per sample was 550K-610K, 98-99% of the reads were mapped successfully to
529 MIT9313 genome yielding mean coverage of 29-42X, 99-100% of the genes had >10X coverage.
530 Mapping quality was assessed using qualimap. SNPs were called only if the read depth was at
531 lease 10 and the Genotype Quality, the Phred-scaled marginal (or unconditional) probability of
532 the called genotype was at least 20. All raw reads can be downloaded from the NCBI Sequence
533 Read Archive under accession numbers PRJNA771345.

534

Acknowledgements

Daniel Segrè and Melisa Osborne for help with sequencing, Sher lab members and especially Natalie Andrawes for help in fluorescence measurements. Hans-Peter Grossart, Zhen Wu and Tal Luzzatto Knaan for critical reading of the manuscript. This work was supported by the Human Frontiers Science Program (grant RGP0020/2016, to DS) and the U.S.-Israel Binational Science Foundation (BSF) - U.S. National Science Foundation (NSF) program in Oceanography (grant 1635070/2016532, to DS). The funders had no role in study design, data collection and analysis, decision to publish, or preparation of the manuscript.

References

Aharonovich, D., & Sher, D. (2016). Transcriptional response of Prochlorococcus to co-culture with a marine Alteromonas: Differences between strains and the involvement of putative infochemicals. *ISME Journal*, *10*(12), 2892–2906. https://doi.org/10.1038/ismej.2016.70

Amin, S. A., Hmelo, L. R., Van Tol, H. M., Durham, B. P., Carlson, L. T., Heal, K. R., Morales, R. L., Berthiaume, C. T., Parker, M. S., Djunaedi, B., Ingalls, A. E., Parsek, M. R., Moran, M. A., & Armbrust, E. V. (2015). Interaction and signalling between a cosmopolitan phytoplankton and associated bacteria. *Nature*, *522*(7554), 98–101. https://doi.org/10.1038/nature14488

Antoniewicz, M. R. (2020). A guide to deciphering microbial interactions and metabolic fluxes in microbiome communities. *Current Opinion in Biotechnology*, *64*, 230–237. https://doi.org/10.1016/j.copbio.2020.07.001

Bagchi, S. N., & Kleiner, D. (1990). Dismutation of hydroxylamine to ammonia and nitrite by a novel, membrane-bound enzyme from the cyanobacterium Phormidium uncinatum. *Biochimica et Biophysica Acta (BBA)/Protein Structure and Molecular*, *1041*(1), 9–13. https://doi.org/10.1016/0167-4838(90)90115-V

Bagchi, S. N., & Kleiner, D. (1991). Interrelationship between hydrogen peroxide, ammonia, glutamine, hydroxylamine and nitrite metabolism in the cyanobacterium Phormidium uncinatum. *Archives of Microbiology*, *156*(5), 367–369. https://doi.org/10.1007/BF00248712

Becker, J. W., Hogle, S. L., Rosendo, K., & Chisholm, S. W. (2019). Co-culture and biogeography of Prochlorococcus and SAR11. *ISME Journal*, *13*(6), 1506–1519. https://doi.org/10.1038/s41396-019-0365-4

Beckett, S. J., Demory, D., Coenen, A. R., Casey, J. R., Dugenne, M., Follett, C. L., Connell, P., Carlson, M. C. G., Hu, S. K., Wilson, S. T., Becker, K. W., Mende, D. R., Armbrust, E. V., White, A. E., Ribalet, F., & Weitz, J. S. (2021). *Diel population dynamics and mortality of Prochlorococcus in the North Pacific Subtropical Gyre*. 1–20.

Biller, S. J., Berube, P. M., Lindell, D., & Chisholm, S. W. (2015). Prochlorococcus: The structure and function of collective diversity. *Nature Reviews Microbiology*, *13*(1), 13–27. https://doi.org/10.1038/nrmicro3378

Biller, S. J., Coe, A., & Chisholm, S. W. (2016). Torn apart and reunited: Impact of a heterotroph on the transcriptome of Prochlorococcus. *ISME Journal*, *10*(12), 2831–2843. https://doi.org/10.1038/ismej.2016.82

Brouwer, A. F., Eisenberg, M. C., Remais, J. V., Collender, P. A., Meza, R., & Eisenberg, J. N. S. (2017). Modeling Biphasic Environmental Decay of Pathogens and Implications for Risk Analysis. *Environmental Science and Technology*, *51*(4), 2186–2196. https://doi.org/10.1021/acs.est.6b04030

Christie-Oleza, J. A., Sousoni, D., Lloyd, M., Armengaud, J., & Scanlan, D. J. (2017). Nutrient recycling facilitates long-term stability of marine microbial phototroph-heterotroph interactions. *Nature Microbiology*, *2*(June). https://doi.org/10.1038/nmicrobiol.2017.100

Cirri, E., & Pohnert, G. (2019). Algae−bacteria interactions that balance the planktonic microbiome. *New Phytologist*, *223*(1), 100–106. https://doi.org/10.1111/nph.15765

Coe, A., Biller, S. J., Thomas, E., Boulias, K., Bliem, C., Dooley, K., Rasmussen, A. N., Legault, K., Keefe, T. J. O., Eric, L., & Chisholm, S. W. (2020). *Coping with darkness: The adaptive response of marine picocyanobacteria to repeated light energy deprivation*. 1–32.

Coe, A., Ghizzoni, J., LeGault, K., Biller, S., Roggensack, S. E., & Chisholm, S. W. (2016). Survival of Prochlorococcus in extended darkness. *Limnology and Oceanography*, *61*(4), 1375–1388. https://doi.org/10.1002/lno.10302

Cole, J. J. (1982). *INTERACTIONS BETWEEN*. 291–314.

Cordero, O. X., Wildschutte, H., Kirkup, B., Proehl, S., Ngo, L., Hussain, F., Le Roux, F., Mincer, T., Polz, M. F., & Roux, F. Le. (2012). Ecological Populations of BacteriaAct as Socially Cohesive Units ofAntibiotic Production and Resistance. *Science (New York, N.Y.)*, *337*(September), 1228–1231. https://doi.org/10.1126/science.1219385

Crane, S. R., & Moore, J. A. (1986). Modeling enteric bacterial die-off: A review. *Water, Air, & Soil Pollution*, *27*(3–4), 411–439. https://doi.org/10.1007/BF00649422

Cubillos-Ruiz, A., Berta-Thompson, J. W., Becker, J. W., Van Der Donk, W. A., & Chisholm, S. W. (2017). Evolutionary radiation of lanthipeptides in marine cyanobacteria. *Proceedings of the National Academy of Sciences of the United States of America*, *114*(27), E5424–E5433. https://doi.org/10.1073/pnas.1700990114

Diner, R. E., Schwenck, S. M., McCrow, J. P., Zheng, H., & Allen, A. E. (2016). Genetic manipulation of competition for nitrate between heterotrophic bacteria and diatoms. *Frontiers in Microbiology*, *7*(JUN). https://doi.org/10.3389/fmicb.2016.00880

Dutkiewicz, S., Follows, M., Marshall, J., & Gregg, W. W. (2001). Interannual variability of phytoplankton abundances in the North Atlantic. *Deep Sea Research Part II: Topical Studies in Oceanography*, *48*(10), 2323–2344.

Field, C. B., Behrenfeld, M. J., Randerson, J. T., & Falkowski, P. (1998). Primary production of the biosphere: Integrating terrestrial and oceanic components. *Science*, *281*(5374), 237–240. https://doi.org/10.1126/science.281.5374.237

Finkel, S. E., & Kolter, R. (1999). Evolution of microbial diversity during prolonged starvation. *Proceedings of the National Academy of Sciences of the United States of America*, *96*(7),

4023–4027. https://doi.org/10.1073/pnas.96.7.4023

Foster, K. R., & Bell, T. (2012). Competition, not cooperation, dominates interactions among culturable microbial species. *Current Biology*, *22*(19), 1845–1850. https://doi.org/10.1016/j.cub.2012.08.005

Fritts, R. K., McCully, A. L., & McKinlay, J. B. (2021). Extracellular Metabolism Sets the Table for Microbial Cross-Feeding. *Microbiology and Molecular Biology Reviews*, *85*(1). https://doi.org/10.1128/mmbr.00135-20

Gau, A. E., Heindl, A., Nodop, A., Kahmann, U., & Pistorius, E. K. (2007). L-amino acid oxidases with specificity for basic L-amino acids in cyanobacteria. *Zeitschrift Fur Naturforschung - Section C Journal of Biosciences*, *62*(3–4), 273–284. https://doi.org/10.1515/znc-2007-3-419

Gralka, M., Szabo, R., Stocker, R., & Cordero, O. X. (2020). Trophic Interactions and the Drivers of Microbial Community Assembly. *Current Biology*, *30*(19), R1176–R1188. https://doi.org/10.1016/j.cub.2020.08.007

Grossart, H. P. (1999). Interactions between marine bacteria and axenic diatoms (Cylindrotheca fusiformis, Nitzschia laevis, and Thalassiosira weissflogii) incubated under various conditions in the lab. *Aquatic Microbial Ecology*, *19*(1), 1–11. https://doi.org/10.3354/ame019001

Grossart, H. P., & Simon, M. (2007). Interactions of planktonic algae and bacteria: Effects on algal growth and organic matter dynamics. *Aquatic Microbial Ecology*, *47*(2), 163–176. https://doi.org/10.3354/ame047163

Grossowicz, M., Roth-Rosenberg, D., Aharonovich, D., Silverman, J., Follows, M. J., & Sher, D. (2017). Prochlorococcus in the lab and in silico: The importance of representing exudation. *Limnology and Oceanography*, *62*(2), 818–835. https://doi.org/10.1002/lno.10463

Hackl, T., Laurenceau, R., Ankenbrand, M. J., Bliem, C., Cariani, Z., Thomas, E., Dooley, K. D., Arellano, A. A., Hogle, S. L., Berube, P., Leventhal, G. E., Luo, E., Eppley, J., Zayed, A. A., Beaulaurier, J., Stepanauskas, R., Sullivan, M. B., DeLong, E. F., Biller, S. J., & Chisholm, S. W. (2021). Novel Integrative Elements and Genomic Plasticity in Ocean Ecosystems. *SSRN Electronic Journal*. https://doi.org/10.2139/ssrn.3817805

Harrington, V., Lau, L., Seddu, K., & Suez, J. (2021). *Ecology and Medicine Converge at the Microbiome-Host*. *6*(4), 4–8.

Hennon, G. M., Morris, J. J., Haley, S. T., Zinser, E. R., Durrant, A. R., Entwistle, E., Dokland, T., & Dyhrman, S. T. (2018). The impact of elevated CO 2 on Prochlorococcus and microbial interactions with â € helper' bacterium Alteromonas. *ISME Journal*, *12*(2), 520–531. https://doi.org/10.1038/ismej.2017.189

Hogg, T., Mechold, U., Malke, H., Cashel, M., & Hilgenfeld, R. (2004). Conformational antagonism between opposing active sites in a bifunctional RelA/SpoT homolog modulates (p)ppGpp metabolism during the stringent response. *Cell*, *117*(1), 57–68. https://doi.org/10.1016/S0092-8674(04)00260-0

Hou, S., López-Pérez, M., Pfreundt, U., Belkin, N., Stüber, K., Huettel, B., Reinhardt, R., Berman-Frank, I., Rodriguez-Valera, F., & Hess, W. R. (2018). Benefit from decline: The primary

transcriptome of Alteromonas macleodii str. Te101 during Trichodesmium demise. *ISME Journal*, *12*(4), 981–996. https://doi.org/10.1038/s41396-017-0034-4

Kettler, G. C., Martiny, A. C., Huang, K., Zucker, J., Coleman, M. L., Rodrigue, S., Chen, F., Lapidus, A., Ferriera, S., Johnson, J., Steglich, C., Church, G. M., Richardson, P., & Chisholm, S. W. (2007). Patterns and implications of gene gain and loss in the evolution of Prochlorococcus. *PLoS Genetics*, *3*(12), 2515–2528. https://doi.org/10.1371/journal.pgen.0030231

Klähn, S., Steglich, C., Hess, W. R., & Hagemann, M. (2010). Glucosylglycerate: A secondary compatible solute common to marine cyanobacteria from nitrogen-poor environments. *Environmental Microbiology*, *12*(1), 83–94. https://doi.org/10.1111/j.1462-2920.2009.02045.x

Koch, H., Dürwald, A., Schweder, T., Noriega-Ortega, B., Vidal-Melgosa, S., Hehemann, J. H., Dittmar, T., Freese, H. M., Becher, D., Simon, M., & Wietz, M. (2019). Biphasic cellular adaptations and ecological implications of Alteromonas macleodii degrading a mixture of algal polysaccharides. *ISME Journal*, *13*(1), 92–103. https://doi.org/10.1038/s41396-018-0252-4

Koch, H., Germscheid, N., Freese, H. M., Noriega-Ortega, B., Lücking, D., Berger, M., Qiu, G., Marzinelli, E. M., Campbell, A. H., Steinberg, P. D., Overmann, J., Dittmar, T., Simon, M., & Wietz, M. (2020). Genomic, metabolic and phenotypic variability shapes ecological differentiation and intraspecies interactions of Alteromonas macleodii. *Scientific Reports*, *10*(1), 1–14. https://doi.org/10.1038/s41598-020-57526-5

Latifi, A., Ruiz, M., & Zhang, C. C. (2009). Oxidative stress in cyanobacteria. *FEMS Microbiology Reviews*, *33*(2), 258–278. https://doi.org/10.1111/j.1574-6976.2008.00134.x

Li, B., Sher, D., Kelly, L., Shi, Y., Huang, K., Knerr, P. J., Joewono, I., Rusch, D., Chisholm, S. W., & Van Der Donk, W. A. (2010). Catalytic promiscuity in the biosynthesis of cyclic peptide secondary metabolites in planktonic marine cyanobacteria. *Proceedings of the National Academy of Sciences of the United States of America*, *107*(23), 10430–10435. https://doi.org/10.1073/pnas.0913677107

Long, R. A., & Azam, F. (2001). Microscale patchiness of bacterioplankton assemblage richness in seawater. *Aquatic Microbial Ecology*, *26*(2), 103–113. https://doi.org/10.3354/ame026103

López-Pérez, M., & Rodriguez-Valera, F. (2016). Pangenome evolution in themarine bacterium alteromonas. *Genome Biology and Evolution*, *8*(5), 1556–1570. https://doi.org/10.1093/gbe/evw098

Malmstrom, R. R., Coe, A., Kettler, G. C., Martiny, A. C., Frias-Lopez, J., Zinser, E. R., & Chisholm, S. W. (2010). Temporal dynamics of Prochlorococcus ecotypes in the Atlantic and pacific oceans. *ISME Journal*, *4*(10), 1252–1264. https://doi.org/10.1038/ismej.2010.60

Mcdonagh, B., Domínguez-Martín, M. A., Gómez-Baena, G., López-Lozano, A., Diez, J., Bárcena, J. A., & García Fernández, J. M. (2012). Nitrogen starvation induces extensive changes in the redox proteome of Prochlorococcus sp. strain SS120. *Environmental Microbiology Reports*, *4*(2), 257–267. https://doi.org/10.1111/j.1758-2229.2012.00329.x

Monod, J. (1949). a Certain Number. *Annual Reviews in M*, *3*(Xl), 371–394.

Moore, L. R., Coe, A., Zinser, E. R., Saito, M. A., Sullivan, M. B., Lindell, D., Frois-Moniz, K.,

Waterbury, J., & Chisholm, S. W. (2007). Culturing the marine cyanobacterium Prochlorococcus. *Limnology and Oceanography: Methods*, *5*(OCT), 353–362. https://doi.org/10.4319/lom.2007.5.353

Moore, S. K., Baird, M. E., & Suthers, I. M. (2006). Relative effects of physical and biological processes on nutrient and phytoplankton dynamics in a shallow estuary after a storm event. *Estuaries and Coasts*, *29*(1), 81–95. https://doi.org/10.1007/BF02784701

Morris, J. J., Johnson, Z. I., Szul, M. J., Keller, M., & Zinser, E. R. (2011). Dependence of the cyanobacterium Prochlorococcus on hydrogen peroxide scavenging microbes for growth at the ocean's surface. *PLoS ONE*, *6*(2). https://doi.org/10.1371/journal.pone.0016805

Morris, J. Jeffrey, Kirkegaard, R., Szul, M. J., Johnson, Z. I., & Zinser, E. R. (2008). Facilitation of robust growth of Prochlorococcus colonies and dilute liquid cultures by "helper" heterotrophic bacteria. *Applied and Environmental Microbiology*, *74*(14), 4530–4534. https://doi.org/10.1128/AEM.02479-07

Morris, J. Jeffrey, Lenski, R. E., & Zinser, E. R. (2012). The black queen hypothesis: Evolution of dependencies through adaptive gene loss. *MBio*, *3*(2), 1–7. https://doi.org/10.1128/mBio.00036-12

Murray A.G. and Parslow J.S. (1999). The analysis of alternative formulations in a simple model of a coastal ecosystem. *Ecological Modelling*, *119*(2–3), 149–166.

Pacheco, A. R., Osborne, M. L., & Segrè, D. (2021). Non-additive microbial community responses to environmental complexity. *Nature Communications*, *12*(1), 1–11. https://doi.org/10.1038/s41467-021-22426-3

Patra, P., & Klumpp, S. (2013). Population Dynamics of Bacterial Persistence. *PLoS ONE*, *8*(5). https://doi.org/10.1371/journal.pone.0062814

Pedler, B. E., Aluwihare, L. I., & Azam, F. (2014). Single bacterial strain capable of significant contribution to carbon cycling in the surface ocean. *Proceedings of the National Academy of Sciences of the United States of America*, *111*(20), 7202–7207. https://doi.org/10.1073/pnas.1401887111

Pruitt, K. M., & Kamau, D. N. (1993). Mathematical models of bacterial growth, inhibition and death under combined stress conditions. *Journal of Industrial Microbiology*, *12*(3–5), 221–231. https://doi.org/10.1007/BF01584194

Ramanan, R., Kim, B. H., Cho, D. H., Oh, H. M., & Kim, H. S. (2016). Algae-bacteria interactions: Evolution, ecology and emerging applications. *Biotechnology Advances*, *34*(1), 14–29. https://doi.org/10.1016/j.biotechadv.2015.12.003

Ratzke, C., & Gore, J. (2017). Modifying and reacting to the environmental pH drives bacterial interactions. *Modifying and Reacting to the Environmental PH Can Drive Bacterial Interactions*, 136838. https://doi.org/10.1101/136838

Rocap, G., Larimer, F. W., Lamerdin, J., Malfatti, S., Chain, P., Ahlgren, N. A., Arellano, A., Coleman, M., Hauser, L., Hess, W. R., Johnson, Z. I., Land, M., Lindell, D., Post, A. F., Regala, W., Shah, M., Shaw, S. L., Steglich, C., Sullivan, M. B., … Chisholm, S. W. (2003). Genome divergence in two Prochlorococcus ecotypes reflects oceanic niche differentiation. *Nature*, *424*(6952), 1042–1047. https://doi.org/10.1038/nature01947

Roth-Rosenberg, D., Aharonovich, D., Luzzatto-Knaan, T., Vogts, A., Zoccarato, L., Eigemann, F., Nago, N., Grossart, H. P., Voss, M., & Sher, D. (2020). Prochlorococcus cells rely on microbial interactions rather than on chlorotic resting stages to survive long-term nutrient starvation. *MBio*, *11*(4), 1–13. https://doi.org/10.1128/mBio.01846-20

Saito, M. A., McIlvin, M. R., Moran, D. M., Goepfert, T. J., DiTullio, G. R., Post, A. F., & Lamborg, C. H. (2014). Multiple nutrient stresses at intersecting Pacific Ocean biomes detected by protein biomarkers. *Science*, *345*(6201), 1173–1177. https://doi.org/10.1126/science.1256450

Schriek, S., Rückert, C., Staiger, D., Pistorius, E. K., & Michel, K. P. (2007). Bioinformatic evaluation of L-arginine catabolic pathways in 24 cyanobacteria and transcriptional analysis of genes encoding enzymes of L-arginine catabolism in the cyanobacterium Synechocystis sp. PCC 6803. *BMC Genomics*, *8*, 1–28. https://doi.org/10.1186/1471-2164-8-437

Segev, E., Wyche, T. P., Kim, K. H., Petersen, J., Ellebrandt, C., Vlamakis, H., Barteneva, N., Paulson, J. N., Chai, L., Clardy, J., & Kolter, R. (2016). Dynamic metabolic exchange governs a marine algal-bacterial interaction. *ELife*, *5*(NOVEMBER2016), 1–28. https://doi.org/10.7554/eLife.17473

Seyedsayamdost, M. R., Case, R. J., Kolter, R., & Clardy, J. (2011). The Jekyll-and-Hyde chemistry of phaeobacter gallaeciensis. *Nature Chemistry*, *3*(4), 331–335. https://doi.org/10.1038/nchem.1002

Seymour, J. R., Amin, S. A., Raina, J. B., & Stocker, R. (2017). Zooming in on the phycosphere: The ecological interface for phytoplankton-bacteria relationships. *Nature Microbiology*, *2*(May). https://doi.org/10.1038/nmicrobiol.2017.65

Sher, D., Thompson, J. W., Kashtan, N., Croal, L., & Chisholm, S. W. (2011). Response of Prochlorococcus ecotypes to co-culture with diverse marine bacteria. *ISME Journal*, *5*(7), 1125–1132. https://doi.org/10.1038/ismej.2011.1

Shoemaker, W. R., Jones, S. E., Muscarella, M. E., Behringer, M. G., Lehmkuhl, B. K., & Lennon, J. T. (2021). Microbial population dynamics and evolutionary outcomes under extreme energy limitation. *Proceedings of the National Academy of Sciences of the United States of America*, *118*(33), 1–8. https://doi.org/10.1073/pnas.2101691118

Steinchen, W., & Bange, G. (2016). The magic dance of the alarmones (p)ppGpp. *Molecular Microbiology*, *101*(4), 531–544. https://doi.org/10.1111/mmi.13412

Teeling, H., Fuchs, B. M., Becher, D., Klockow, C., Gardebrecht, A., Bennke, C. M., Kassabgy, M., Huang, S., Mann, A. J., Waldmann, J., Weber, M., Klindworth, A., Otto, A., Lange, J., Bernhardt, J., Reinsch, C., Hecker, M., Peplies, J., Bockelmann, F. D., … Amann, R. (2012). Substrate-controlled succession of marine bacterioplankton populations induced by a phytoplankton bloom. *Science*, *336*(6081), 608–611. https://doi.org/10.1126/science.1218344

Ting, C. S., Hsieh, C., Sundararaman, S., Mannella, C., & Marko, M. (2007). Cryo-electron tomography reveals the comparative three-dimensional architecture of Prochlorococcus, a globally important marine cyanobacterium. *Journal of Bacteriology*, *189*(12), 4485–4493. https://doi.org/10.1128/JB.01948-06

Tolonen, A. C., Aach, J., Lindell, D., Johnson, Z. I., Rector, T., Steen, R., Church, G. M., & Chisholm, S. W. (2006). Global gene expression of Prochlorococcus ecotypes in response to changes in nitrogen availability. *Molecular Systems Biology*, *2*. https://doi.org/10.1038/msb4100087

Ustick, L. J., Larkin, A. A., Garcia, C. A., Garcia, N. S., Brock, M. L., Lee, J. A., Wiseman, N. A., Keith Moore, J., & Martiny, A. C. (2021). Metagenomic analysis reveals global-scale patterns of ocean nutrient limitation. *Science*, *372*(6539), 287–291. https://doi.org/10.1126/science.abe6301

Van Boekel, M. A. J. S. (2002). On the use of the Weibull model to describe thermal inactivation of microbial vegetative cells. *International Journal of Food Microbiology*, *74*(1–2), 139–159. https://doi.org/10.1016/S0168-1605(01)00742-5

Vetsigian, K., Jajoo, R., & Kishony, R. (2011). Structure and evolution of streptomyces interaction networks in soil and in silico. *PLoS Biology*, *9*(10). https://doi.org/10.1371/journal.pbio.1001184

Warringer, J., Anevski, D., Liu, B., & Blomberg, A. (2008). Chemogenetic fingerprinting by analysis of cellular growth dynamics. *BMC Chemical Biology*, *8*, 1–10. https://doi.org/10.1186/1472-6769-8-3

Weisskopf, L., Schulz, S., & Garbeva, P. (2021). Microbial volatile organic compounds in intra-kingdom and inter-kingdom interactions. *Nature Reviews Microbiology*, *19*(6), 391–404. https://doi.org/10.1038/s41579-020-00508-1

Yelton, A. P., Acinas, S. G., Sunagawa, S., Bork, P., Pedrós-Alió, C., & Chisholm, S. W. (2016). Global genetic capacity for mixotrophy in marine picocyanobacteria. *ISME Journal*, *10*(12), 2946–2957. https://doi.org/10.1038/ismej.2016.64

Zheng, Q., Wang, Y., Lu, J., Lin, W., Chen, F., & Jiao, N. (2020). Metagenomic and metaproteomic insights into photoautotrophic and heterotrophic interactions in a Synechococcus culture. *MBio*, *11*(1). https://doi.org/10.1128/mBio.03261-19

Zoccarato, L., Sher, D., Miki, T., Segrè, D., & Grossart, H. P. (2020). Comparative whole-genome approach to identify traits underlying microbial interactions. *BioRxiv*, 1–53. https://doi.org/10.1101/2020.06.30.179929